Shall We Dance? How A Multicopper Oxidase Chooses Its Electron Transfer Partner

LILIANA QUINTANAR,[†] CHRISTOPHER STOJ,[‡] ALEXANDER B. TAYLOR,[§] P. JOHN HART,[§] DANIEL J. KOSMAN,*[,⊥] AND EDWARD I. SOLOMON[||]

School of Medicine and Biomedical Sciences, The University at Buffalo, Buffalo, New York 14214, Departamento de Química, Centro de Investigación y de Estudios Avanzados (Cinvestav), 07360 México, D.F., Mexico, Department of Chemistry, Biochemistry and Biophysics, Niagara University, Niagara University, New York 14109, Department of Biochemistry, University of Texas Health Science Center, San Antonio, Texas 78229, and Department of Chemistry, Stanford University, Stanford, California 94305

Received February 7, 2007

ABSTRACT

Multicopper oxidases (MCOs) are encoded in the genomes of Eukarya, Bacteria, and Archea. These proteins are unique in that they contain at least four Cu atom prosthetic groups organized into one each of the three spectral classifications of copper sites in biology: type 1 (T1), type 2 (T2), and binuclear type 3 (T3), where the T2 and T3 sites form a trinuclear Cu cluster. With these four redox-active copper sites, the multicopper oxidases catalyze the four-electron ($4e^-$) reduction of dioxygen to $2H_2O$, an activity that they alone share with the terminal heme-containing oxidases. Most MCOs exhibit broad specificity towards organic reductants, while a relatively small number of family members exhibit equally robust activity towards metal ions like Fe^{II}, Cu^{I}, and Mn^{II} and, thus, are considered metallo-oxidases. This Account analyzes the structure–activity features of multicopper oxidases that determine their relative substrate specificity. Since the substrate oxidation step involves an outer-sphere electron transfer from the reductant to the T1Cu site in the protein, the concepts of Marcus theory are applied to unravel the origin of the substrate specificity of the multicopper ferroxidases.

A little examined aspect of biological catalysis is the mechanism(s) by which essential transition metal ions are reduced and oxidized. Certainly for aerobic organisms, these reactions are critical to metal homeostasis because aerobes are confronted with higher valent states, commonly exchange inert metal ion valence states, and utilize these metals in their lower valent forms. This pattern is exemplified by iron and copper; aerobic organisms first reduce the Fe^{III} and Cu^{II} found in the environment to Fe^{II} and Cu^{I}, in most cases via the activity of a heme-containing metalloreductase. These lower valent ions are then substrates for a variety of permeases, metallochaperones, or both but ultimately undergo a re-oxidation in the course of their metabolism. In iron metabolism, the oxidative half of this cycle is sometimes catalyzed by multicopper oxidases (MCOs) with specific activity towards Fe^{II}. This Account summarizes our understanding of the structure and function relationships in MCOs that lead to this metabolically critical but heretofore poorly understood specificity.

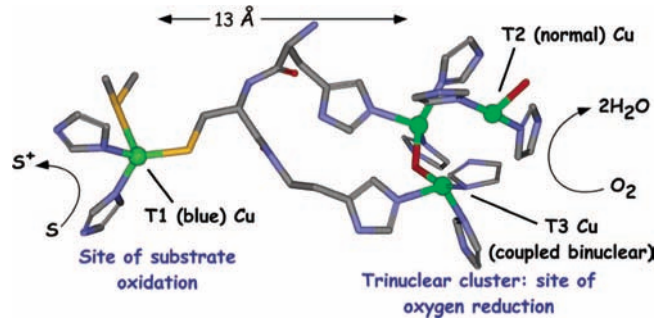

FIGURE 1. Active site of the multicopper oxidases. Cu sites are shown in green spheres. Figure generated from the crystal structure of ascorbate oxidase (pdb accession number 1AOZ).[6]

An Introduction to Multicopper Oxidases

The MCOs are a family of enzymes that couple the one-electron oxidation of four substrate equivalents with the four-electron reduction of O_2 to H_2O.[1] The catalytic motif in these proteins includes at least four Cu atoms that are classified into three types of sites (Figure 1): type 1 Cu^{II} (T1Cu); type 2 (T2) Cu^{II}, with an electronic structure comparable to simple planar Cu^{II} complexes; and the type 3 (T3) binuclear Cu^{II}–Cu^{II} cluster, which is diamagnetic because the coppers are antiferromagnetically coupled

* Corresponding author. Department of Biochemistry, 140 Farber Hall, 3435 Main St., Buffalo, NY 14214, 716-829-2842 (phone), 716-829-2661 (fax), camkos@buffalo.edu (e-mail).

[†] Centro de Investigación y de Estudios Avanzados (Cinvestav).

[‡] Niagara University.

[§] University of Texas Health Science Center.

[⊥] The University at Buffalo.

[||] Stanford University.

Liliana Quintanar received her Ph.D. from Stanford University, where she studied bioinorganic chemistry. After a postdoctoral fellowship at the Department of Neurochemistry of Instituto de Fisiología Celular, UNAM, she is now Assistant Professor at the Department of Chemistry of Cinvestav (Mexico), where she studies metal neurotoxicity.

Christopher S. Stoj received his Ph.D. degree from the University at Buffalo examining ferroxidase structure–function relationships. He is currently an Assistant Professor of Biochemistry in the Department of Biochemistry, Chemistry, and Physics at Niagara University.

Alexander B. Taylor received his Ph.D. degree from the University of Texas at Austin. He is now the Technical Director of the X-ray Crystallography Core Laboratory at the University of Texas Health Science Center at San Antonio.

P. John Hart received his Ph.D. from the University of Texas at Austin. He is the Ewing Halsell, President's Council Distinguished Professor of Biochemistry and the Director of the X-Ray Crystallography Core Laboratory at the University of Texas Health Science Center at San Antonio.

Daniel J. Kosman received his Ph.D. from the University of Chicago. He is now Professor of Biochemistry at the University of Buffalo where his group focuses on ferroxidases and the cellular trafficking of iron.

Edward I. Solomon received his Ph.D. from Princeton University and was a Postdoctoral Fellow at the Ørsted Institute of the University of Copenhagen and at Caltech. He was a Professor at MIT and is now the Monroe E. Spaght Professor at Stanford University. His research focuses on physical–inorganic, bioinorganic, and theoretical–inorganic chemistry.

10.1021/ar600051a CCC: $37.00
Published on Web 04/11/2007

through a hydroxide bridge.[3] The type 2 and type 3 sites form a trinuclear Cu cluster, which is the site of oxygen reduction.[2]

The main electron transfer (ET) steps in the reaction mechanism of MCOs are (i) reduction of the T1Cu site by the substrate, (ii) ET from the T1Cu site to the trinuclear cluster, and (iii) O_2 reduction by the trinuclear cluster.[4] Thus, the main functional role of the T1Cu site is to shuttle electrons from the substrate to the trinuclear Cu cluster site over a distance of ~13 Å (Figure 1). Its coordination sphere always contains two histidine ligands and one cysteine; the latter forms a very covalent Cu–S bond with an intense $S_{Cys} \rightarrow Cu^{II}$ charge transfer band at ~600 nm and leads to the characteristic blue color of the MCOs.[1,5] The covalency of the T1Cu site facilitates ET to the trinuclear Cu cluster through a cysteine–histidine protein pathway (Figure 1).

The multicopper oxidases are present in several organisms.[1] They are important for lignin formation in plants (plant laccases); pigment formation, lignin degradation, and detoxification processes in fungi (fungal laccases); iron metabolism in yeast (Fet3p)[7,8] and mammals (hCp and hephaestin); copper homeostasis in bacteria (CueO);[9] and manganese oxidation by bacterial spores (MnxG).[10] Therefore, the physiological substrates of the multicopper oxidases vary from organic compounds to metal ions like Fe^{II}, Cu^{I},[11] and Mn^{II}.

Most MCOs can use a wide variety of aromatic phenols and amines as reducing substrates,[1] while a few exhibit an equally robust activity towards Fe^{II}, Cu^{I}, or Mn^{II}. The latter group includes Cp and Fet3p in Eukarya and CueO in Bacteria, but it is likely that several other metallooxidases exist in pro- and eukaryotic genomes. Since substrate oxidation occurs via the T1Cu, substrate specificity is conferred by structure–activity relationships near this site and not at the trinuclear cluster. Therefore, the substrate of T1Cu ET step of the MCO reaction is the focus of the remainder of this Account.

Examining the MCO Type 1 Cu Site: Electronic Structure and Reduction Potential

The T1Cu coordination sphere can come with or without an axial methionine residue; archived laccase (Lc) sequences divide roughly 50:50 in this respect. A four-coordinate T1Cu site, as found in ascorbate oxidase (AO), tree laccases, and the two redox-active T1 sites in human Cp (hCp), involves short Cu–S_{Cys} and long Cu–S_{Met} bonds (Figure 2A). In the fungal laccases, Fet3p and the redox-inactive T1Cu site in hCp,[12] the absence of a methionine ligand results in a shift of the Cu atom into the N_{His}–N_{His}–S_{Cys} plane and a trigonal planar geometry (Figure 2B). Spectroscopic studies of the T1Cu site in fungal laccases have shown an increased covalency of the Cu–S_{Cys} bond and ligand field strength, compared with the classic blue Cu site in plastocyanin.[13] Thus, in Fet3p and the fungal laccases, the Cu–S_{Cys} bond strength compensates for the lack of an axial ligand.

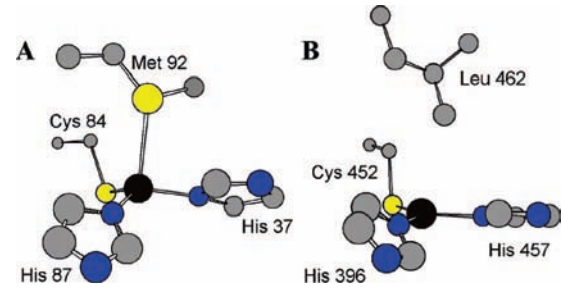

FIGURE 2. The four-coordinate T1Cu site in plastocyanin (A) and the trigonal planar T1Cu site in *Coprinus cinereus* laccase (B). Figure generated from the crystal structures (accession numbers 1PLC[15] and 1HFU,[16] respectively).

Table 1. Comparison of Reduction Potentials of MCO T1Cu Sites[a]

MCO	$E°$ (mV vs NHE)
T1Cu Sites with Axial Methionine Ligand	
Cucurbita pepo medullosa AO	344
Rhus vernicifera laccase	434
human ceruloplasmin (redox active T1Cu's)	448
Polyporous pinsitus laccase F463M mutant	680
T1Cu Sites without Axial Methionine Ligand	
Saccharomyces cerevisiae Fet3p	427
Coprinus cinereus laccase	550
Polyporus pinsitus laccase, wild-type	770
Polyporus versicolor laccase[b]	778
human ceruloplasmin (T1 in domain 2)	≥1000

[a] Adapted from ref 14. [b] *Polyporus versicolor* laccase is also known as *Trametes versicolor* laccase (*Tv*Lc).

The relationship between T1 site ligation, electronic structure, and reduction potential ($E°$) has been a subject of extensive examination.[5] The reduction potentials for the T1Cu sites in MCOs vary from 0.34 V in *Cucurbita pepo medullosa* AO to 0.79 V in *Trametes versicolor* laccase (*Tv*Lc) (Table 1). Overall, the three-coordinate T1 sites of fungal laccases exhibit substantially higher reduction potentials than four-coordinate T1 sites. Site-directed mutagenesis has been used to evaluate the role of the T1Cu axial ligand in tuning the $E°$ of the site.[13] Conversion of the three-coordinate T1Cu site in *Polyporous pinsitus* laccase into a four-coordinate site in the F463M mutant reduces its $E°$ from 780 to 680 mV (Table 1). Similarly, mutation of the axial methionine ligand of the T1Cu sites in azurin, cucumber stellacyanin, nitrite reductase, and rusticyanin to non-coordinating groups results in an increase in $E°$ of the T1 site of 80–130 mV.[5] Thus, the presence of the methionine ligand contributes to a decrease of ~100 mV in the reduction potential, given that the remaining protein environment is kept constant.

A methionine axial ligand is present in most of the metazoan MCOs that are likely to be ferroxidases, while in fungal ferroxidases the T1Cu sites are three-coordinate. For the three-coordinate T1Cu sites in Fet3p and the fungal laccases, the $E°$ ranges from 430 to 790 mV, yet the geometric and electronic structure of their T1 sites are comparable.[13,14] Conversely, the multicopper ferroxidases Fet3p and hCp exhibit similar substrate specificity and comparable $E°$ (430 mV), yet the former has a three-coordinate T1Cu site, while the redox-active T1 sites of hCp have methionine ligands.[14] Clearly, there are other

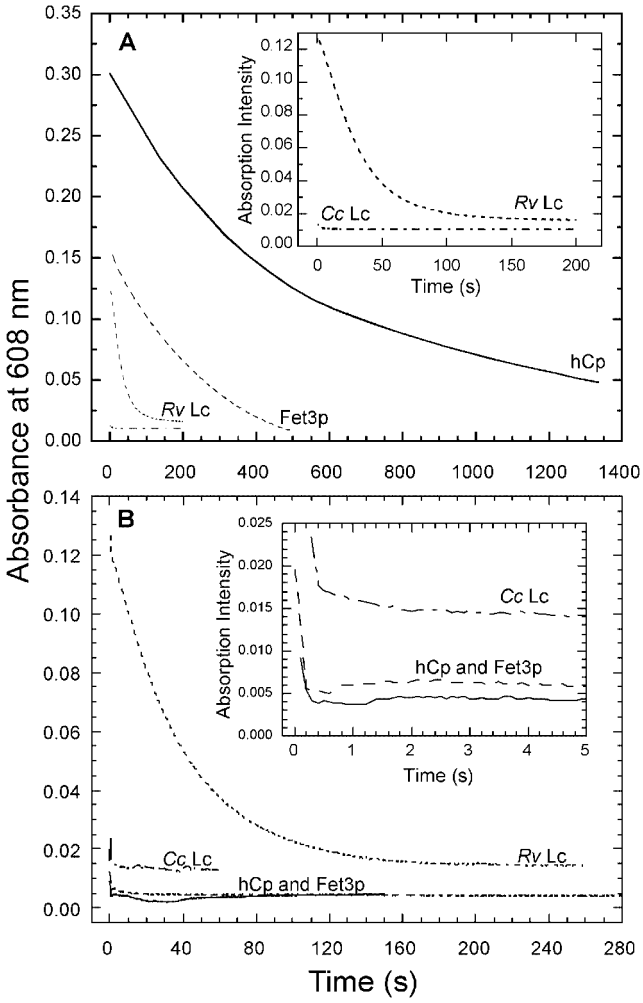

FIGURE 3. T1Cu^{II} reduction kinetics in laccases and ferroxidases: (A) reduction of the T1Cu sites of hCp (—), Fet3p (– – –), *Rv*Lc (- - -), and *Cc*Lc (– - –) with hydroquinone; (B) reduction of the same proteins by Fe^{II}. Note the 5-fold difference in the time scales. While Fet3p and hCp are the slowest in their reduction by hydroquinone (A), they are both completely reduced by Fe^{II} within 2 ms (B). Figures reprinted with permission from ref 14. Copyright 2001 American Chemical Society.

factors, such as solvent accessibility, dipole orientation, and H-bonding, that contribute to the tuning of reduction potentials.

Reactivity and Specificity of the T1Cu Site: Fingerprinting MCOs

The reactivity of the T1Cu site can be probed by following the bleaching of the 600 nm band upon addition of reductant. Figure 3 shows that *Rhus vernicifera* laccase (*Rv*Lc), *Coprinus cinereus* laccase (*Cc*Lc), Fet3p and hCp exhibit differential reactivity towards 1,4-hydroquinone (Figure 3A) and Fe^{II} (Figure 3B).[14] While the reduction of the T1Cu sites in Fet3p, hCp, and *Cc*Lc by Fe^{II} is extremely fast, *Rv*Lc is at least 4 orders of magnitude slower (Figure 3B, Table 2). In contrast, in the reduction kinetics of the T1Cu sites by 1,4-hydroquinone, *Cc*Lc showed the fastest reduction: >2-fold faster than *Rv*Lc, which in turn is 10-fold faster than Fet3p, which in turn is 10-fold faster than hCp. Note that the T1Cu sites in *Rv*Lc, Fet3p, and hCp have essentially identical reduction potentials (~440 mV; Table 1), yet strikingly different rates of reduction by organic versus metallo-reductants. This example illustrates that the driving force provided by the $E°$ of the T1Cu is not a strong predictor of substrate specificity and that other factors must be considered.

The differential reactivity of the T1Cu sites in these enzymes can be analyzed in terms of the semiclassical theory for the rate of intermolecular ET, k_{ET}, which is described by eq 1.[17]

$$k_{ET} = K_A S\sqrt{4\pi^3/(h^2\lambda k_B T)}(H_{DA})^2\, e^{[-(\Delta G° + \lambda)^2/(4\lambda k_B T)]} \quad (1)$$

Here, K_A is the equilibrium formation constant for the electron donor–acceptor complex, S is a steric term that grades how appropriate the donor–acceptor complex is for ET; λ is the reorganization energy associated with the valence change at the donor and acceptor sites, $\Delta G°$ is the electrochemical driving force, and H_{DA} is the electronic matrix coupling element that quantifies the efficiency of a given ET pathway from the donor to the acceptor.

*Rv*Lc is comparably slow with Fe^{II} and bulky organic reductants like hydroquinone, while *Cc*Lc is fast with both substrates. The reactivity difference between *Rv*Lc and *Cc*Lc can be ascribed to several factors in eq 1. The T1Cu site in *Cc*Lc is more oxidizing than that in *Rv*Lc by ~150 mV (Table 1), and being a three-coordinate and more covalent site, the *Cc*Lc site will have a smaller reorganization energy, which would increase k_{ET}. However, the differences in $\Delta G°$ and λ cannot account for the >1000-fold faster rate of reduction observed for *Cc*Lc in comparison to *Rv*Lc; thus, the relative contributions of other factors must be considered. The binding of an organic substrate to *Cc*Lc can be inferred by comparison to the structures of two other fungal laccases: *Tv*Lc[18] and *Melanocarpus albomyces* laccase.[19] In both proteins, one of the two T1Cu histidine ligands is solvent exposed at the bottom of a shallow cleft, where the substrate can bind in possible H-bond contact with the histidine Nε2; this has been demonstrated in *Tv*Lc. The structure of the *Tv*Lc complex with 2,5-xylidine suggests that amino group H-bonding to the protein contributes to ligand binding and indicates that a typical phenolic substrate would bind similarly via the D206 carboxylate and the H458 Nε2 hydrogen. The structure of this donor–enzyme complex is consistent with the relatively rapid ET observed with *Cc*Lc: substrate oriented for productive ET (favorable S) in H-bond contact with a T1Cu ligand (favorable H_{DA}). Since there is no crystal structure of *Rv*Lc, it is not possible to assess the contributions of S and H_{DA} to the rate of reduction. However, it is clear that *Cc*Lc exhibits faster k_{ET} than *Rv*Lc due to a significantly more solvent-exposed T1Cu site (K_A), a more favorable substrate–enzyme orientation (S), and a more direct ET pathway into the T1Cu site (H_{DA}).

In contrast to the *Cc*Lc and *Rv*Lc case, Fet3p and hCp exhibit little difference in rate for a given substrate; they are both equally fast (≥1200 s^{-1}) for reduction by Fe^{II}, while the rate of reduction of Fet3p by 1,4-hydroquinone

Table 2. T1Cu^{II} Reduction Rates and Substrate Specificity[a]

MCO	k_{Fe}, reduction by Fe^{II} (s^{-1})	k_{HQ}, reduction by hydroquinone (M^{-1} s^{-1})[b]	k_{Fe}/k_{HQ} (M) relative effective $[Fe^{II}]$[c]
Rhus vernicifera Lc	0.026	3.9×10^6	6.7×10^{-9}
Coprinus cinereus Lc	>1200	$>8.6 \times 10^{6c}$	$>1.4 \times 10^{-4}$
Fet3p	>1200	3.5×10^5	$>3.4 \times 10^{-3}$
hCp	>1200	6.1×10^4	$>1.9 \times 10^{-2}$

[a] Data taken from ref 14. [b] Second-order rate constant. [c] Estimated value based on the lower limit for k_{obs} at the lowest hydroquinone concentration employed.

is only 10-fold faster than that for hCp (Table 2). The redox potentials of the T1Cu sites in these enzymes are approximately the same (430–450 mV; Table 1). Their difference in reactivity towards 1,4-hydroquinone has thus been explained in terms of the accessibility of their T1Cu sites.[14] The crystal structure of hCp[20,21] shows that the redox-active T1Cu sites are buried ~10 Å beneath the surface, at the bottom of a long, narrow, highly negatively charged channel, limiting access by bulky organic substrates. On the other hand, the crystal structure of Fet3p[22] shows a more solvent-accessible T1 site, which facilitates the formation of the substrate–enzyme complex (*S* and K_A terms) and possibly shortens the ET pathway (increasing H_{DA}), thus explaining its 10-fold faster rate of reduction by 1,4-hydroquinone compared with hCp.

From Figure 3, it becomes evident that hCp and Fet3p exhibit substrate specificity for Fe^{II}. The origin of this specificity has been subject for discussion. Early crystallographic studies of hCp[20] suggested the presence of one divalent metal ion binding site in the vicinity of each redox-active T1Cu site.[23] The recent crystal structure of Fet3p confirmed the presence of an Fe-binding site similar to that of hCp.[22] Thus, Fet3p is similar to hCp in that it possesses an Fe-binding site that confers this enzyme with substrate specificity for Fe^{II}. However, Fet3p shares more sequence homology to fungal laccases than to hCp; in fact, it has a three-coordinate T1Cu site as all fungal laccases do, while the T1Cu in hCp is four-coordinate. Thus, Fet3p could be described as a fungal laccase adapted to perform ferroxidase chemistry, and the comparison of the structures of *Tv*Lc and Fet3p can highlight the features that differentiate a laccase from a ferroxidase.

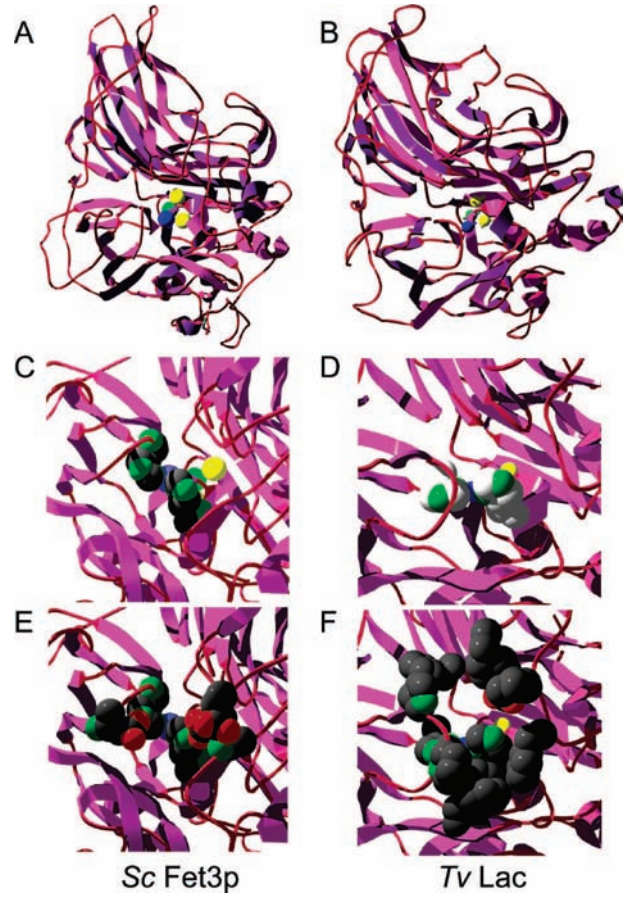

FIGURE 4. Ribbon diagrams for Fet3p (A) and *Tv*Lc (B) illustrate that the overall folding of the two proteins is indistinguishable.[18,22] The strand topology is illustrated together with the ligating histidine imidazole side chains (C, D). Although the T1Cu sites are similar, a loop in *Tv*Lc blocks solvent accessibility to H395. Inclusion of the side chains of the surrounding amino acid residues (E and F) explains the structural origin of the specificity of the two enzymes. In Fet3p (E), acidic residues E185, D409, and D283 shield the imidazoles H489 and H413 from solvent, while in *Tv*Lc (F), the T1 site is lined with nonpolar side chains including F162, L164, F239, F265, F332, F337, P394, and P397.

Laccases versus Ferroxidases

The cupredoxin folds of *Tv*Lc[18] and Fet3p[22] are clearly evident and render the two proteins virtually indistinguishable (Figure 4A,B). However, the protein fold around the T1Cu sites in the two proteins is significantly different and provides the basis for their substrate specificity. The T1Cu site in *Tv*Lc (Figure 4C) is shallow with few steric constraints for substrate binding, while the site in Fet3p (Figure 4D) is more structurally defined, particularly by acidic side chains like E185, D283, and D409, which confer to the T1 site a negatively charged surface (Figure 4E). In *Tv*Lc, the organic substrate binds to one of the T1Cu histidine ligands via a H-bond with its Nε2 NH (Figure 5A), while in Fet3p, E185 and D409 "mask" the two T1Cu histidine ligands (Figures 4E and 5B): the E185 Oε2 is H-bonded to the H489 Nε2, while the D409 Oδ2 is H-bonded to the corresponding nitrogen of H413. This distinction in second-sphere coordination dictates the connectivity between the substrate and the T1 site and, therefore, how the electron is transferred from the substrate to the T1Cu^{II}. The Fet3p structure suggests that these glutamic acid and aspartic acid residues may be the signature motifs of a multicopper ferroxidase.

Analysis of the MCO sequences shows that residues E185 and D409 are completely conserved in the multicopper ferroxidases and absent in the fungal laccases (Table 3). Particularly striking is the complete conservation in all MCOs (both ferroxidases and laccases) of the

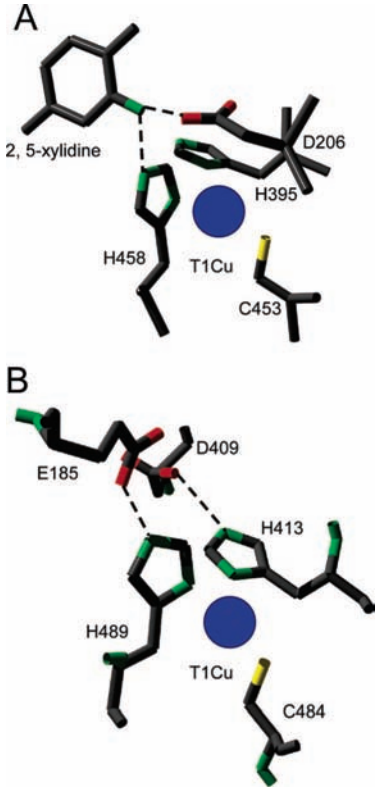

FIGURE 5. Hydrogen-bond networks at the T1Cu distinguish a *Tv*Lc (A) from the ferroxidase Fet3p (B). Binding of the substrate analog, 2,5-xylidine, at the T1 site in *Tv*Lc (A) involves H-bonds to D206 and to one of the NE2 pyrrole nitrogens of H458, a ligand to the T1Cu.[18] In Fet3p (B), both histidine ligands to the T1Cu, His489 and His413, are H-bonded to carboxylate side chains of E185 and D409, respectively.[22]

Table 3. Sequence Comparison of Four Fungal Ferroxidases and Two Fungal Laccases[a]

		E185	D283	D409	
Ferroxidases					
ScFet3p	NP	TGA**E**PIPQNL	DDTML**D**VIPSD	NNQ**D**TGT	HPFHLHG
ScFet5p	NP	TGA**E**PIPQNI	DETML**D**VVPPE	NNY**D**SGR	HPFHLHG
SpFio1	NP	TGA**E**PVPDTG	DESLF**D**TIP-D	DNH**D**TGK	HPFHLHG
CaFet3p	NP	TGA**E**PIPQNF	DTTML**D**SVPAD	NNF**D**TGK	HPFHLHG
Laccases					
TvLac	DA	TLINGLGRSA	NLTVIEVDGIN	ALAP-GA	HPFHLHG
MaLac	TQ	NNAPPFSDNV	SLVNHTMTVIA	PEGPFSL	HPMHLHG

[a] *Sc*, *Saccharomyces cerevisiae*; *Sp*, *Schizosaccharomyces pombe*; *Ca*, *Candida albicans*; *Tv*, *Trametes versicolor*; *Ma*, *Melanocarpus albomyces*.

HPFHLHG motif that includes three histidine ligands to the Cu atoms in these proteins, in contrast to the lack of homology in the sequences that include three conserved acidic residues (E185, D409, and D283 in Fet3p). These differences are reflected in the structures of Fet3p and the fungal *Tv*Lc. The conformation of the two T1Cu coordinating histidines is identical in the two proteins (Figure 4C,D), but the polypeptide strands framing them are different. The H413/H395 strand in Fet3p is short and contains D409, which is poised to be H-bonded to the H413 Nε2; while in *Tv*Lc this strand is longer and serves as a flap that blocks access to the H395 NH moiety. As to the strands that frame the H489/H458, in Fet3p this strand loops over H489 (Figure 4C,E) and contains E185, which is H-bonded to the H489 Nε2; while in *Tv*Lc the conformation pulls the chain back exposing the H458 Nε2 fully to solvent (Figure 4D,F), and it contains nonpolar residues appropriate for binding of large nonpolar reductants. Finally, the loop that includes D283 in Fet3p extends into the site, bringing D283 along with it; while in *Tv*Lc, this loop is short and pulled back leaving plenty of room for the docking of a bulky organic reductant.

Thus, the active site in the ferroxidase Fet3p is distinguished from that in *Tv*Lc in three ways: (1) it is spatially more constrained and has a negative (instead of a nonpolar) electrostatic surface; (2) the Nε2 NH groups of the T1Cu histidine ligands are not solvent-exposed and therefore not easily accessible to reducing substrates; and (3) each of the two pyrrole NH groups is in H-bond contact with a carboxylate group (E185 or D409), which in turn is solvent-exposed and thereby accessible for interaction with a metallosubstrate. The contributions of this structural arrangement to the ferroxidase activity of Fet3p have been analyzed through site-directed mutagenesis, magnetic circular dichroism (MCD), and kinetic studies, as discussed below.

Probing Fe(II) Binding Sites in the Multicopper Ferroxidases: Contributions to Reactivity

The notion that the E185, D409, and D283 residues play an important role in Fe^{II} oxidation is confirmed by reductive half-reaction and steady-state turnover kinetic studies.[24–26] While the reduction of the T1Cu site in wild-type Fet3p by Fe^{II} is very fast (k_{obs} > 1200 s^{-1}, Table 2), mutations at the E185, D409, and D283 residues cause a significant decrease in rate (Table 4). This is consistent with steady-state turnover kinetics that show an increase in the Michaelis–Menten constant for Fe^{II} for all variants (Table 4), indicating a decrease in affinity for Fe^{II}. The largest effect is observed upon elimination of the carboxylate moiety at the E185 position.

The presence of an Fe^{II} binding site in Fet3p was first probed using magnetic circular dichroism (MCD) in the near-IR region, where non-heme Fe^{II} sites exhibit ligand field transitions.[24] MCD studies showed that Fe^{II} binds to Fet3p with high affinity, yielding a signal at ~8900 cm^{-1} (Figure 6). The E185A mutation shifts this signal to ~9700 cm^{-1}, where Fe^{II} in buffer solution absorbs, indicating that the high-affinity Fe^{II} binding is abolished by this mutation. In contrast, the MCD spectrum of Fe^{II} bound to E185D Fet3p (Figure 6) indicates that the high-affinity Fe(II) binding is conserved when a shorter carboxylate moiety is retained at the E185 position. Thus, MCD titrations demonstrate that the carboxylate moiety at the E185 position plays a critical role in high-affinity Fe^{II} binding to Fet3p.

MCD analysis indicates that Fe^{II} bound to Fet3p is six-coordinate.[24] Similar MCD studies with hCp have identified comparable Fe^{II} binding sites. The hCp crystal structure suggests the participation of three carboxylates and one histidine residue in the Fe^{II} coordination envi-

Table 4. Redox and Kinetic Properties of Wild-Type and Mutant Fet3 Proteins[a]

Fet3p species	T1 redox potential (mV)	Michaelis–Menten constants for HQ K_M (mM) k_{cat} (min^{-1})	Michaelis–Menten constants for Fe^{II} K_M (μM) k_{cat} (min^{-1})	first-order rate constants for T1Cu reduction by Fe^{II} (k_{ET}, s^{-1})
WT	433	25.5 ± 2.5 131.3 ± 5.0	4.9 ± 1.8 40.1 ± 1.4	≥1200
E185D	434	8.2 ± 1.1 94.3 ± 4.3	8.6 ± 1.2 32.0 ± 3.0	141 ± 7.0
E185A	433	18.2 ± 1.5 91.7 ± 2.6	35.6 ± 2.8 24.3 ± 0.6	7.8 ± 0.2
D283A	439	19.3 ± 1.1 169.5 ± 3.5	19.3 ± 1.5 75.7 ± 1.9	681.9 ± 23.7
D409A	550	30.3 ± 2.4 139.7 ± 4.7	18.8 ± 1.6 48.2 ± 1.2	62.03 ± 0.60
E185A/D409A	549	30.5 ± 2.1 132.8 ± 3.9	3994 ± 387 13.9 ± 0.4	0.41 ± 0.01

[a] Data taken from refs 24–26.

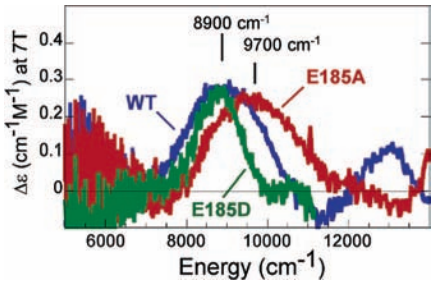

FIGURE 6. Fe^{II} binding to Fet3 proteins, followed by near-IR MCD. Spectra of reduced Fet3p wt (blue), E185D (green), and E185A (red) with 1 equiv of Fe^{II}. Fe^{II} does not bind to the E185A protein, but it does bind to Fet3p wt and E185D. Figure adapted with permission from ref 24. Copyright 2004 American Chemical Society.

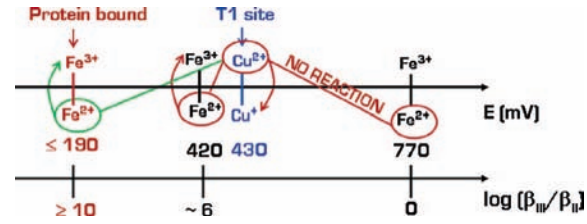

FIGURE 7. Tuning of the $E°$ of the Fe^{II} substrate in the multicopper ferroxidases. Reaction of the T1Cu site ($E° = 430$ mV) with aqueous Fe^{II} at pH = 0 ($E° = 770$ mV) would not proceed, while at pH = 6.5 ($E°(Fe^{II}/Fe^{III}) = 420$ mV), this reaction would have a very small thermodynamic force. Thus, the $E°$ of the protein-bound Fe must be ≤190 mV for its reaction with the T1Cu site to be stoichiometric. According to the expression $E°_{aqueous} - E°_{protein} = 59 \log(\beta_{III}/\beta_{II})$, this corresponds to a ratio of affinities for Fe^{III} and Fe^{II} $\beta_{III}/\beta_{II} \geq 10^{10}$, where β_{III} and β_{II} are the equilibrium constants for the formation of the Fe^{III}–protein and Fe^{II}–protein complexes, respectively.

ronment.[20] Thus, hCp-bound Fe^{II} can be reasonably described as a six-coordinate site with three monodentate carboxylates, one histidine, and two water molecules.[24] In light of the recent crystal structure of Fet3p, it has become clear that E185, D409, and D283 participate in Fe^{II} binding to this protein.[22] Consistently, the E185A, D409A, and D283A mutants display practically no Fe uptake *in vivo*, and turnover kinetic experiments show that the mutation of these carboxylate residues to alanine leads to an increase in the Michaelis–Menten K_M for Fe^{II} (Table 4). This effect is particularly strong in the E185A mutant, which shows the largest increase in K_M, implying a significant decrease in SK_A and explaining the dramatic decrease in the rate of T1Cu reduction by Fe^{II} observed for this mutant (Table 4). Thus, one of the main contributions of these carboxylate residues is to provide a coordination environment for high-affinity binding of the Fe^{II} substrate.

Another important contribution of the Fe^{II} binding sites in Fet3p and hCp is their ability to tune the $E°$ of the bound iron. The T1Cu sites in these ferroxidases have a redox potential of ~430 mV, while that for aqueous Fe^{II} is 420 mV at pH 6.5; thus, the $1e^-$ ET to the $T1Cu^{II}$ is not thermodynamically favorable. However, these enzymes are fully reduced by stoichiometric Fe^{II}, suggesting that the $E°$ of *protein-bound* Fe^{II} must be decreased to an *upper* limit of 190 mV (Figure 7) For hCp-bound or Fet3p-bound Fe^{II} to exhibit a $E°$ of ~190 mV, the ratio of the affinities of these proteins for Fe^{III} and Fe^{II} must be $\sim 10^{10}$ (Figure 7). Overall, oxygen donor ligands stabilize Fe^{III} more than Fe^{II}; the stability constants of dicarboxylic ligands for Fe^{III} can be 4–10 orders of magnitude higher than those for Fe^{II}. In ferric-binding proteins, like transferrins, high affinity for Fe^{III} is achieved by using oxygen donor ligands and by neutralizing the metal charge with exogenous anions.[27] Thus, the $E°$ for Fet3p-bound Fe is tuned down, such that it is significantly below the $E°$ of the T1Cu site, supplying sufficient driving force for this ET reaction. Note that this tuning of the substrate's $E°$ is only required in the *ferroxidase* reaction; the potentials for aromatic reductants are generally <200 mV. Thus, the carboxylate residues at the Fe^{II} binding sites in the multicopper ferroxidases also play an important role in providing the driving force for ET to the T1Cu site.

Finally, a third factor that contributes to the rate of ET from the Fe^{II} substrate to the T1Cu site is the H_{DA} term. In this regard, the Fe^{II} binding sites in Fet3p and hCp are optimized for efficient ET pathways. In the crystal structure of hCp, three main ET pathways have been identified,[14,24] the most efficient being through E272, which is part of the Fe^{II} binding site and is H-bonded to one of the T1Cu histidine ligands. The recent crystal structure of Fet3p[22] shows that the E185 and D409 residues exhibit a similar connectivity to each of the T1Cu histidine ligands: the

E185 Oε2 is H-bonded to the H489 Nε2, while the D409 Oδ2 is H-bonded to the corresponding nitrogen of H413 (Figures 4E and 5B). Therefore, the E185 and D409 residues not only contribute to the high affinity for Fe^{II} (increasing SK_A) and help tune the Fe^{II} redox potential (increasing ΔG°) but also provide efficient ET pathways into the T1Cu site, increasing H_{DA}. It is not surprising then, that mutating these residues to alanine yields large decreases in the rates of T1Cu reduction by Fe^{II} (Table 4). This is particularly striking in the E185A/D409A mutant, which highlights the important contributions of these two residues to k_{ET}.

The notion that the E185 residue plays an important role in ET into the T1Cu site is illustrated by the E185D protein, which exhibits no change in the T1Cu E° (no change in ΔG°) and conserves high-affinity Fe^{II} binding (same SK_A) yet shows a decrease in T1Cu reduction rate compared with wild-type. The main effect of the E185D mutation is likely the loss of the E185/H489 pathway: a shorter carboxylate residue would perturb the H-bonding connectivity to H489, and D409/H413 would provide the most competent ET pathway. Eliminating the E185/H489 pathway is calculated to decrease k_{ET} by 1 order of magnitude, consistent with the $\geq$10 fold decrease in T1Cu reduction rate observed for the E185D mutant (Table 4). Thus, the decrease in rate for this mutant mostly reflects the loss of an efficient ET pathway.

In summary, systematic deletions of the three carboxylates in Fet3p that primarily distinguish it as a ferroxidase have shed light into how the multicopper ferroxidases achieve their substrate specificity towards Fe^{II}. The protein fold around the T1Cu site is rich in carboxylate residues that (i) provide a coordination environment for high-affinity binding of Fe^{II}, (ii) tune the reduction potential of the bound iron to afford a large driving force for Fe^{II} oxidation, and (iii) provide efficient pathways for ET into the T1Cu site.

Concluding Remarks

A subset of the MCO family has diverged from the rest to adapt its reactivity towards a new cohort of substrates, lower valent first row transition metals ions. In order to achieve this metallo-oxidase activity, these MCOs have engineered a substrate binding site that maximizes each of the factors that contribute to ET from the metal ion substrate to the T1Cu site. Our work highlights the fact that, while binding and orienting the substrate, these metallo-oxidases also tune the reduction potential of the protein-bound metal ion and provide the electron-coupling pathways for its oxidation. Thus, the use of a combination of spectroscopic studies and single and steady-state turnover kinetic experiments, blended with concepts that quantitatively describe the free energy landscape for ET has lead to a mechanistic understanding of the biologic redox cycling of transition metals. Further insight into the specificity of the MCOs will certainly derive from analogous studies on other metallo-oxidases of this family, including CueO[9] and MnxG,[28] which possess Cu^I and Mn^{II} oxidase activity, respectively.

This research was supported by NIH Grants DK31450 (to E.I.S.) and DK53820 (to D.J.K.) and R. A. Welch Foundation Grant AQ-1399 (to P.J.H.).

References

(1) Solomon, E. I.; Sundaram, U. M.; Machonkin, T. E. Multicopper oxidases and oxygenases. *Chem. Rev.* **1996**, *96*, 2563–2605.
(2) Allendorf, M. D.; Spira, D. J.; Solomon, E. I. Low temperature MCD studies of native laccase: Spectroscopic evidence for exogenous ligand bridging at a trinuclear copper active site. *Proc. Natl. Acad. Sci. U.S.A.* **1985**, *82*, 3063–3067.
(3) Malkin, R.; Malmström, B. G. The State and function of copper in biological systems. *Adv. Enzymol.* **1970**, *33*, 177–244.
(4) Solomon, E. I.; Chen, P.; Metz, M.; Lee, S. K.; Palmer, A. E. Oxygen binding, activation, and reduction to water by copper proteins. *Angew. Chem., Int. Ed.* **2001**, *40*, 4570–4590.
(5) Solomon, E. I.; Szilagyi, R. K.; George, S. D.; Basumallick, L. Electronic structures of metal sites in proteins and models: contributions to function in blue copper proteins. *Chem. Rev.* **2004**, *104*, 419–458.
(6) Messerschmidt, A.; Ladenstein, R.; Huber, R.; Bolognesi, M.; Avigliano, L.; Petruzzelli, R.; Rossi, A.; Finazzi-Agro, A. Refined crystal structure of ascorbate oxidase at 1.9 Å resolution. *J. Mol. Biol.* **1992**, *224*, 179–205.
(7) de Silva, D. M.; Askwith, C. C.; Eide, D.; Kaplan, J. The FET3 gene product required for high affinity iron transport in yeast is a cell surface ferroxidase. *J. Biol. Chem.* **1995**, *270*, 1098–1101.
(8) Askwith, C.; Eide, D.; Van Ho, A.; Bernard, P. S.; Li, L.; Davis-Kaplan, S.; Sipe, D. M.; Kaplan, J. The FET3 gene of *S. cerevisiae* encodes a multicopper oxidase required for ferrous iron uptake. *Cell* **1994**, *76*, 403–410.
(9) Rensing, C.; Grass, G. *Escherichia coli* mechanisms of copper homeostasis in a changing environment. *FEMS Microbiol. Rev.* **2003**, *27*, 197–213.
(10) Francis, C. A.; Casciotti, K. L.; Tebo, B. M. Localization of Mn(II)-oxidizing activity and the putative multicopper oxidase, MnxG, to the exosporium of the marine *Bacillus* sp. strain SG-1. *Arch. Microbiol.* **2002**, *178*, 450–456.
(11) Stoj, C.; Kosman, D. J. Cuprous oxidase activity of yeast Fet3p and human ceruloplasmin: implication for function. *FEBS Lett.* **2003**, *554*, 422–426.
(12) Machonkin, T. E.; Zhang, H. H.; Hedman, B.; Hodgson, K. O.; Solomon, E. I. Spectroscopic and magnetic studies of human ceruloplasmin: identification of a redox-inactive reduced type 1 copper site. *Biochemistry* **1998**, *37*, 9570–9578.
(13) Palmer, A. E.; Randall, D. W.; Xu, F.; Solomon, E. I. Spectroscopic studies and electronic structure description of the high potential type 1 copper site in fungal laccase: Insight into the effect of the axial ligand. *J. Am. Chem. Soc.* **1999**, *121*, 7138–7149.
(14) Machonkin, T. E.; Quintanar, L.; Palmer, A. E.; Hassett, R.; Severance, S.; Kosman, D. J.; Solomon, E. I. Spectroscopy and reactivity of the type 1 copper site in Fet3p from *Saccharomyces cerevisiae*: Correlation of structure with reactivity in the multicopper oxidases. *J. Am. Chem. Soc.* **2001**, *123*, 5507–5517.
(15) Guss, J. M.; Bartunik, H. D.; Freeman, H. C. Accuracy and precision in protein structure analysis: restrained least-squares refinement of the structure of poplar plastocyanin at 1.33 Å resolution. *Acta Crystallogr.* **1992**, *B48*, 790–811.
(16) Ducros, V.; Brzozowski, A. M.; Wilson, K. S.; Ostergaard, P.; Schneider, P.; Svendson, A.; Davies, G. J. Structure of the laccase from *Coprinus cinereus* at 1.68 Å resolution: Evidence for different 'type 2 Cu-depleted' isoforms. *Acta Crystallogr., Sect. D: Biol. Crystallogr.* **2001**, *57*, 333–336.
(17) Marcus, R. A.; Sutin, N. Electron transfer in chemistry and biology. *Biochim. Biophys. Acta* **1985**, *811*, 265–322.
(18) Bertrand, T.; Jolivalt, C.; Briozzo, P.; Caminade, E.; Joly, N.; Madzak, C.; Mougin, C. Crystal structure of a four-copper laccase complexed with an arylamine: Insights into substrate recognition and correlation with kinetics. *Biochemistry* **2002**, *41*, 7325–7333.
(19) Hakulinen, N.; Kiiskinen, L. L.; Kruus, K.; Saloheimo, M.; Paananen, A.; Koivula, A.; Rouvinen, J. Crystal structure of a laccase from *Melanocarpus albomyces* with an intact trinuclear copper site. *Nat. Struct. Biol.* **2002**, *9*, 601–605.
(20) Lindley, P. F.; Card, G.; Zaitseva, I.; Zaitsev, V.; Reinhammar, B.; Selin-Lindgren, E.; Yoshida, K. An X-ray structural study of human ceruloplasmin in relation to ferroxidase activity. *J. Biol. Inorg. Chem.* **1997**, *2*, 454–463.

(21) Zaitseva, I.; Zaitsev, V.; Card, G.; Moshkov, K.; Bax, B.; Ralph, A.; Lindley, P. The X-ray structure of human ceruloplasmin at 3.1 Å: Nature of the copper centres. *J. Biol. Inorg. Chem.* **1996**, *1*, 15–23.
(22) Taylor, A. B.; Stoj, C. S.; Ziegler, L.; Kosman, D. J.; Hart, P. J. The copper-iron connection in biology: Structure of the metallo-oxidase Fet3p. *Proc. Natl. Acad. Sci. U.S.A.* **2005**, *102*, 15459–15464.
(23) hCp contains three T1Cu sites, one of them is three-coordinate, it has a high reduction potential, and it is permanently reduced, while the other two are four-coordinate and redox-active. The latter two are comparable in structure, and each has an Fe binding site in its vicinity (see ref 12).
(24) Quintanar, L.; Gebhard, M.; Wang, T. P.; Kosman, D. J.; Solomon, E. I. Ferrous binding to the multicopper oxidases Saccharomyces cerevisiae Fet3p and human ceruloplasmin: contributions to ferroxidase activity. *J. Am. Chem. Soc.* **2004**, *126*, 6579–6589.
(25) Stoj, C.; Augustine, A. J.; Zeigler, L.; Solomon, E. I.; Kosman, D. J. The structural basis of the ferrous iron specificity of the yeast ferroxidase Fet3p. *Biochemistry* **2006**, *45*, 12741–12749.
(26) Wang, T.-P.; Quintanar, L.; Severance, S.; Solomon, E. I.; Kosman, D. J. Targeted suppression of the ferroxidase and iron trafficking activities of the multicopper oxidase, Fet3p, from *Saccharomyces cerevisiae*. *J. Biol. Inorg. Chem.* **2003**, *8*, 611–620.
(27) Taboy, C.; Vaughan, K.; Mietzner, T.; Aisen, P.; Crumbliss, A. Fe^{3+} coordination and redox properties of a bacterial transferrin. *J. Biol. Chem.* **2001**, *276*, 2719–2724.
(28) Francis, C. A.; Tebo, B. M. Enzymatic manganese(II) oxidation by metabolically dormant spores of diverse *Bacillus* species. *Appl. Environ. Microbiol.* **2002**, *68*, 874–880.

AR600051A